Whistler Mode Waves in the Jovian Magnetosheath

Naiguo Lin[1], P. J. Kellogg[1], J. P. Thiessen[1],

D. Lengyel-Frey[2], B. T. Tsurutani[3], J. L. Phillips[4]

[1] School of Physics and Astronomy, University of Minnesota, Minneapolis, MN 55455.

[2] Department of Astronomy, University of Maryland, College Park, MD 20'742.

[3] JPL, California Institute of Technology, Pasadena, CA 91109.

[4] Los Alamos National Laboratory, Los Alamos, NM 87545.

Submitted to the Journal of Geophysical Research

April, 1994

Abstract

During the Ulysses flyby of Jupiter in February, 1992, the spacecraft traversed the Jovian magnetosheath for a few hours during the inbound pass and for a few days during the outbound pass. Burst-1ike electromagnetic waves at frequencies of $\sim 0.1 - 0.4$ of the local electron cyclotron frequency have been observed by the unified radio and plasma wave (URAP) experiment. The waves were more often observed in the regions which were probably the outer or middle magnetosheath, especially near the bow shock, and rarely seen in the magnetosphere/magn etosheath boundary layer. The propagation angle of the waves are estimated by comparing the measurements of the wave electric and magnetic fields on the spin plane with the corresponding values calculated using the cold plasma dispersion relation under local field and plasma conditions. It is found that the waves may propagate obliquely with wave angles between $\sim$ 30°--50°. These waves are likely to be the whistler mode waves which are excited by suprathermal electrons with a few hundred eV and a slight anisotropy ($T_\perp / T_\parallel \sim 1.1 - 1.5$). They are probably similar in nature to the lion roars observed in the Earth's magnetosheath. Signature of coupling between the mirror mode and the whistler mode have also been observed. 'l'he plasma conditions which favor the excitation of the whistler mode instability during the wave events exist as observed by the plasma experiment of Ulysses.

Introduction

Early spacecraft missions have observed sporadic bursts of magnetic emissions in the Earth's magnetosheath [*Smith et al.*, 1967, 1969], which were reported as a characteristic feature of the magnetosheath and known as 'lion roars'. The waves which have frequencies of about one half of the local electron cyclotron frequency, f_{ce}, occurred when the ambient magnetic field decreased, and disappeared when the field magnitude recovered [*Smith and Tsurutani, 1976*], It has been suggested that the emissions are whistler mode waves propagating nearly along the ambient magnetic field. Later observat ions of the magnetosheath by ISEE spacecraft detected similar electromagnetic noise which coupled with drift mirror waves [*Thorne and Tsurutani, 1981; Anderson et al., 1982; Tsurutani et aL, 1982*]. It is suggested that the lion roars originate by cyclotron resonant instability with anisotropic magnetosheath electrons when the magnetic energy pcr particle, $B_0^2/8\pi N$, where B_0 is the magnitude of the ambient magnetic field and N is the number density of the plasma, falls to values close or below the electron thermal energy. The generation of low B high N regions by the drift mirror inst ability leads to the electrons becoming cyclotron unstable.

The existence of whistler mode waves in the Jovian magnetosphere has long been studied to account for sporadic decameter radiation from Jupiter [*Chang, 1963*], and to explain the observed distribution of the energetic electrons in the inner Jovian magnetosphere (see, for example, *Sentman and Goertz, 1978*, and references therein). It is suggested th at the pitch angle scattering of energetic electrons by whistler mode waves sets the limit of the intensity of the energetic electron flux in the equatorial region of Jupiter's inner magnetosphere, which is a similar mechanism proposed for the Earth's case [*Kennel and Petschek*, 1966]. Later observations by the Voyager spacecraft have demonstrated the existence of several types of whistler mode waves which include auroral hiss, chorus, and lightning-generated whistlers (see review by *Scarf et al.*, 1981;

Gurnett and Scarf, 1983). These whistler mode emissions were detected in the inner Jovian magnetosphere, especially near the Io torus.

During the Ulysses flyby of Jupiter in February 1992, whistler mode waves have been observed when the spacecraft passed through the 10 torus region from $\sim 48°$ North to $\sim 33°$ South magnetic latitude [*Stone et al., 1992a*; Farrell *et al., 1993a, b*]. They have been identified as auroral hiss from the Io torus (named "tororal" hiss by *Farrell et al. [1993b]),* and plasm aspheric-like hiss, both of which have also been observed by the Voyager spacecraft.. Owing to its unique orbit which passed through high magnetic latitude regions, Ulysses has discovered solar wind driven aurora] hiss at very high latitudes which resembles the funnel-shaped whistler-mode auroral hiss observed at high latitudes around the Earth.

Ulysses spent several hours during the inbound pass and a few days during the outbound pass in the Jupiter's magnetosheath region, and thus provided a good opportunity to examine the occurrence of plasma waves in the region which had not been much explored previously. This paper will report the observations of whistler mode waves in the Jovian magnetosheath which in nature are probably similar to those observed in the Earth's magnetosheath as lion roam.

Instrumentation and Observations

The plasma wave data used in this study were obtained by two separate instruments of the URAP experiment: the waveform analyser (WFA) with 22 channels between 0.08 and 448 Hz, and the fast envelope sampler (FES). Both instruments measure magnetic as well as electric field components. The FES provides rapid samples (up to 1.1 msec sampling period) of rectified signal in a selected bandwidth detected by one of the four antennas (E_x, E_z, B_y, B_z). It takes 26 min at a bit rate of 1024 to read out an event of approximat ely a one secon d period. The FES data used in this study are magnetic

signals measured by the B_y antenna that rotates in the spin plane. The filter bandwidth had been selected at 0.01-1 kHz. The WFA data used arc 64 sec averages of electric and magnetic field measured in the spin plane, denoted as E_{xy} and B_{xy}, respectively. Data of field component along the spin axis, E_z and B_z, are contaminated by interference with another instrument for the periods of interest and thus are not used. A brief description of the two instruments can be found in *Lin et al. [1993]* for WFA, and in *Kellogg et al.* [1992] for FES. A detailed description of the URAP experiment has been presented by *Stone et al.* [1992 *b*].

The trajectory of Ulysses during the flyby of Jupiter is shown in Figure 1 in fixed magnetic dipole frame. Ulysses first crossed the Jupiter$s bow shock in the morning sector at 1733 UT of Feb 2, 1992 and entered the magnetosheath. It crossed the Jovian magnetopause about four hours later and entered the Jupiter's magnetosphere. Due to the contraction of the magnetosphere, the spacecraft again entered the magnetosheath and traveled in the region including the magnetosheath/magnetosphere boundary layer for another 11 hours or so until it entered the Jovian magnetosphere at 0400 UT, Feb 4. During the outbound pass, the spacecraft, traveling at magnetic latitudes between $\sim$ –25° and $\sim$ --45°, went into the dusk flank of the thick Jovian magnetosheath. Due to the compression and expansion motions of the Jovian magnetosphere, Ulysses went into and out of the magnetosheath several times from 0024, Feb 12 to 0753, Feb 16, including two bow shock crossings at 0037 and 0428 of Feb 14, and the last exit into the solar wind. A detail summary of the timing of bow shock, magnetopause, and magnetosheath crossings can be found in Table 1 of *Phillips et al. [1 993].* In this study we have followed their identification of the magnctoshcath, boundary layer, and magnetosphere regions and the entry and exit times, but include the magnetopause boundary layer as part of the magnetosheath region.

Jupiter's magnetosheath region is more quiet compared to the magnetosphere as

observed by the URAP plasma wave instruments. Plasma waves above the local plasma frequency at several kHz, which are believed to be the escaping Jovian continuum radiation [*Kaiser et al.*, 1994], arc commonly seen in the magnetosheath. There is also electromagnetic noise below the local electron cyclotron frequency but well above the proton cyclotron frequency detected by the WFA instrument, although less frequently. The focus of this study will be on the low frequency plasma waves. We have excluded in this study the wave events right at the four bow shock crossings which will be studied separately.

In Figure 2 we display the 64 scc averaged magnetic wave intensity measured in the spin plane in 5 channels between 9.3 and 37 Hz for *a,* inbound magnetosheath passes and *b,* outbound magnetosheath passes. Burst-like magnetic noise can be seen during the magnetosheath passes (marked with solid bars in the top panels of each plot), mostly in the periods close to the bow shock crossings: between ~ 1730 and 2130 of day 33 (Feb 2); 0600 of day 44 (Feb 13) and 0030 of day 45; 0400 and 0800 of day 45; and 0400 and 0800 of day 47. We note that in most of the above intervals (except for the early part of the interval on day 44), Ulysses was within 2 to 3 R_J from the location of the bow shock at crossing times, On day 43, between 1400 and 2000, wave bursts are also seen, This is a period when wave bursts are seen that apparently arc far from the bow shock. In the rest of the magnetosheath periods, including the one in days 34/35, and the entire day 46, little magnetic noise was detected. The above occurrence distribution of the magnetic noise seems to suggest that the region near to the bow shock favors the excitation of these low frequency waves, but wc cannot justify it since wc do not know the time variation of the bow shock location. The above wave bursts arc also seen in the corresponding electric field data (not shown) at the same periods.

A sample period is shown in Figure 3a and 3*b* to take a close look at these electro-

magnetic bursts. Figure 3a show the same magnetic field data as in Figure 2 but for the period of 0400 to 0800 of day 45, for the first four high-band channels of WFA only, while Figure 3*b* is the corresponding spin plane electric field power density. Besides the bursts near 0430 which are associated with a bow shock crossing due to an expansion of the Jovian magnetosphere, there are several bursts near 0520, 0555, and 0620. Corresponding peaks of these bursts can be found in the electric field data. We have taken six 3 intervals (0505-0518, 0520-0529, 0529-0540,0550-0600, 0615-0625, and 0645-0655) in this period for further analysis. A total of 26 such intervals of wave events in the entire magnetosheath passes of Ulysses has been analyzed in this study.

A power spectra covering a frequency range between 0.22 Hz and 34,5 kHz obtained from the WFA and the plasma frequency receiver (PFR) which cover a frequency range between 578 Hz ancl 34.5 kHz for the interval between 0520 and 0529 of day 45 is shown in Figure 3c. The upper panels show the relative intensity of the electric signal (left) and magnetic signal (right) which is defined as the received signals subtracted by the background noise level of the instrument and then divided by the noise level, Both the signals and noise levels are plotted in the lower panels. The upper panels of the figure clearly show a peak at 10 to 20 Hz for both electric and magnetic waves, The ambient magnetic field strength for this interval is $\sim$ 3.6 nT. Thus the peak frequency of the waves is about 0.1-0.2 times the local electron cyclotron frequency. These waves have also been detected independently by the FES instrument, Figure *3d* displays the magnetic wave intensity recorded by the FES for a 1 sec period at 0520:27 of day 45, when we see a power peak in the 14 Hz Channel in Figure 3a at about the same time. The FES record clearly shows a modulation of the rectified magnetic signal at about 16 Hz. The :maximurn amplitude of the waves in the FES data ($\sim 1\,0^{-2}$ nT) is larger than that derived from the WFA data ($\sim 1.30\ 10^{-3}$ nT) because the WFA data are an average over a much longer time period (64 see).

Some wave events have a shorter duration than theories shownin Figure 3 and look more spike-like. Figure *4a* and *b* show spin plane B and E fields for a period on day 4'7 (Feb 16), 1992, between 0300 and 0700, in which three intervals were chosen as wave events (0400-041 O, 0505-0515, and 0620-0630). The wave burst in the first event is spike-like with a peak frequency in the 3'7 Hz channel, as shown in the spectra in Figure 4c. 'J'his peak frequency is about 0.33 times the local electron cyclotron frequency. The electric wave data for this interval contain a larger electrostatic component, and are more noisy than corresponding magnetic wave data, A peak at about 10 kHz in the electric wave spectra (upper panel of Figure 4c) are probably the escaping continuum radiation above the plasma frequency. The low frequency magnetic wave event was also captured by tlhc FES, and is shown in Figure *4d*, which displays a clear modulation at 38.3 Hz.

Only 9 out of 26 of the wave events selected were captured by the FES and show periodic magnetic field variation. This is because the operating FES channel is switched between B_y and E_z antennas. Only in about 36 out of 97 hours of magnetosheath periods was tlhe FES connected to the B_y antenna. The electric signals are usually noisy containing more components stronger than the ones we are interested in, and thus the low frequency modulation superimposed by stronger signals is not seen in the electric field record. Also, in the FES data, selection process, stronger noise will replace weaker events in the memory. A 26 min period is needed for one readout which is much longer than the duration of a wave burst (presumably only a few seconds). The long period of the process and replacement of weaker signals by stronger ones may cause the FES to miss the low frequency wave bursts recorded in the WFA data.

Analysis and Discussion

All low frequency wave events observed in the [illegible] with obvious elcctro-

magnetic signatures have peak frequencies of ~ 10 — 40 Hz, a fraction of the local electron gyrofrequency, but well above the proton cyclotron frequency ($f_{cp} << f < f_{ce}$). For these intervals of wave events, the observed magnetosheath electron density is $\sim 0.1 - 1\ /cm^3$, with the energy of bulk electrons about a few tens of eV, and the ambient magnetic field is a few nT. Under such cold plasma conditions, the electromagnetic waves that propagate are most likely to be whistler mode waves.

Propagation Angles of the Waves

Most of the whistler mode waves that occur in the Earth's magnetosheath, lion roars, are found to propagate at small angles (< 30°) to the ambient magnetic field [*Smith and Tsurutani, 1976*]. The wave angle, θ of whistler mode waves can be calculated from the dispersion relation if one knows the wave index of refraction, n, which satisfies

$$n^2 \simeq \frac{\omega_{pe}^2}{\omega(\Omega_e Cos\ \theta - \omega)}$$

where ω, ω_{pe}, and Ω_e are the wave frequency, electron plasma frequency, and electron cyclotron frequency, respectively. The ratio cB/E, where c is the speed of light, and B and E are the magnitudes of the wave magnetic and electric fields, respectively, is often used to estimate the wave refractive index, but such estimation is true for parallel propagating waves only [*Lengyel-Frey et al.*, 1994]. Since we have measurements of E and B in the spin plane only, we cannot calculate the refractive index directly from the data. *Lengyel-Frey et al.* [1994] have developed a technique for determining the whistler propagation angle from the observed magnetic and electric field amplitude ratio. We have adapted their method to analyze our wave events. The idea is to compare the ratio of the observed B to E on the spin plane, cB_{xy}/E_{xy}, with the corresponding values calculated from the dispersion relation under observed plasma conditions and given wave angles. The wave angle for which the calculated ratio matches the observed

ratio is then taken as the propagation angle of the wave.

In a wave coordinate system $x_0y_0z_0$ in which the Z. axis is parallel to the ambient magnetic field and the wave normal is in the x_0 - z_0 plane, the wave electric and magnetic field can be expressed as [*Mosier and Gurnett*, 1971]:

$$E_{x0} = E_0 \cos(-\omega t)$$

$$E_{y0} = \left(\frac{D}{S - n^2}\right) E_0 \sin(-\omega t)$$

$$E_{z0} = -\frac{n^2 \cos\theta \sin\theta}{(P - n^2 \sin^2\theta)} E_0 \cos(-\omega t)$$

and

$$B_{x0} = -\frac{n \cos\theta}{c} \left(\frac{D}{S - n^2}\right) E_0 \sin(-\omega t)$$

$$B_{y0} = \frac{n \cos\theta}{c} \frac{P}{(P - n^2 \sin^2\theta)} E_0 \cos(-\omega t)$$

$$B_{z0} = \frac{n \sin\theta}{c} \frac{D}{(S - n^2)} E_0 \sin(-\omega t)$$

where E_0 is an arbitrary value for electric field strength, and S, P, and D are the dielectric tensor elements defined by *Stix* [1 962]. Our measurements are made in the spacecraft coordinates xyz. This system can be transformed to the wave coordinates $x_0y_0z_0$ through the following rotations (see Figure 5): first rotate the coordinates around z axis by an angle α to $x'y'z'(z' = z)$, so that the ambient magnetic field **B**. lies on the x' -- z' plane, then rotate the coordinates $x'y'z'$ around y' by an angle γ to $x''y''z''(y'' = y')$ so that the z" axis aligned with B_o, and finally, rotate $x''y''z''$ around the z" axis by a δ angle into the wave coordinates $x_0y_0z_0(z_0 = z")$, so that the wave vector **k** lies on the x_0z_0 plane, The detail of the transformation is presented and discussed in *Lengyel-Frey et al.* [1994],

For a given wave angle θ, knowing the ambient magnetic field and electron density, we may calculate the wave refractive index n and, using the above expressions, the three

components of the wave electric and magnetic fields in the wave coordinates $x_0y_0z_0$, keeping the constant E_0. These components can be transformed into the spacecraft coordinates if the values of angles α, γ, and δ are given. The δ angle is unknown, while the angles 7 and α can be determined from the observed background magnetic field: $7 = \cos^{-1}(B_{0z}/|\mathbf{B}.|)$, and $\alpha = \tan^{-1} B_{0y}/B_{0z}$, where B_{0z}, B_{0y}, B_{0z} arc t hrec components of **B.** in the spacecraft coordinates.

In our analysis, for each data point in a wave interval, we calculated three components of **E** and **B** in the wave coordinate system for 100 values of θ between 0° and the resonance cone angle, $\theta_{res} = \cos^{-1}(\omega/\Omega_e)$, and then transformed the components to the spacecraft coordinates by giving 18 values of δ ranging from 0° to 180°. The ambient magnetic field and the plasma, density for the interval are obtained from the magnetometer data and the solar wind plasma experiment data. The peak frequency seen in the spectra is taken as the wave frequency. For each θ and δ, the ratio cB_{xy}/E_{xy} in spacecraft coordinates, where $B_{xy} = \sqrt{\overline{B_x^2} + \overline{B_y^2}}$ and $E_{xy} = \sqrt{\overline{E_x^2} + \overline{E_y^2}}$, is calculated, and then is compared with the ratio obtained from WFA data, Those wave angles for which the calculated ratios agree with the observed ratio within a certain limit are select ed, and the average of them is then taken as the propagation angle of the wave. The limit is set arbitrarily as ≤ 2, which is within about 1% of the observed cB_{xy}/E_{xy} values.

Figure 6 show an example of the results of such analysis for the interval 0520-0529 of day 45. The wave frequency is taken as 14.0 Hz, the peak channel in the WFA spectra, which is also consistent with the FES data. The average of the observed cB_{xy}/E_{xy} over this interval is ~ 290. There are 9 out of 10 data points which have θ angle determined. The θ values range from $\sim 25°$ to 50° with an average of 37.4°. We have analyzed all 26 wave intervals and found the wave angles determined are generally large, between 30° and $\sim$ 60°, in contrast with those of Earth's lion roars which arc less than 30°.

Energy and Anisotropy of Resonant Electrons

The whistler mode instability can be excited by electrons whose parallel velocity Doppler-shifts the wave frequency to their cyclotron frequency. Only electrons with a certain energy can satisfy the resonance condition $k \cdot v = \omega + m\Omega_e$, where m is an integer O or -11. The resonance energy for the whistler mode instability can be expressed as

$$E_{res} = \frac{B_0^2}{8\pi N} \frac{\Omega_e}{\omega \cos^2 \theta} (\cos\theta - \frac{\omega}{\Omega_e})(m + \frac{\omega}{\Omega_e})^2.$$

The Landau resonance (m = O case) is nearly always be damping for an electron distribution that decreases monotonically ***[Kennel, 1966]*** which is generally true in our case. Thus for all wave events, we have estimated the electron energy required for the principal cyclotron resonance ($m = -1$). The resonance with m = +1 usually required much higher energy. In the previous example, 0520-0529 of day 45, taking the wave frequency f =14.0 Hz, and the wave angle θ = 37.4°, the resonance energy is calculated as ~ 48.3 eV, comparable to the energy of thermal electrons. In all 26 events, the calculated resonance energies fall between ~ 30 – 1000 eV, with most of them at several tens of eV to a few hundred eV. The solar wind plasma experiment data show that in the magnetosheath region, a typical electron energy spectra have a peak count rate at tens of eV [*Phillips et al., 1993].* Sufficient fraction of electrons at several tens of eV to a few hundred eV for cyclotron resonance is likely to exist, evidence of which will be discussed in the following paragraph. It is interesting to notice that, in Plate 1 of *Phillips et al.* [1993], the energy of the bulk electrons on day 45 is shown gradually decreasing from near 100 eV before 0700 to about 10 CV after 0900, which implies a reduction in the suprathermal electron population. Coincidently, the whistler wave activity for the same period weakened and disappeared at about 0800 (see Figure 2*b*). Similar correlation is also seen during the inbound pass. Wave activity disappeared

after 2200, day 33, when the energy of the bulk electrons decreased and thus the numbers of suprathermal electrons (not shown in *Phiillips et al.),* This correlation is consistent wit h the observed whistler waves being excited by the resonance with the suprathermal electrons,

The growth rate of the whistler mode depends on competition between Landau and cyclotron reson antes. The Landau damping becomes more dominant for larger wave angles [*Kennel,* 1966]. To keep the wave growth for a large wave angle, a certain number of electrons at cyclotron resonance is necessary. The harder the energy spectrum of electrons is, the larger the propagation angle is allowed to have wave growth. For example, *Kennel [1966]* has shown that for a wave at ω/Ω_e = 1/9, which is similar to our m agnetosheath waves, an electron distribution with a power law spectrum $1/E^2$ would allow wave growth taking place out to $\theta \sim 40°$. In the Jovian magnetosheath, electron distribution with energy spectra $1/E^2$ or harder has been observed [*Phillips et al., 1993].* For example, near 0451 of day 45 (see Figure 4 of *Phillips et al.*), the distribution of electrons between 17.5 eV and 157 CV (or electron speed 2500 km/s to 7500 km/s in their figure) is higher than $\sim 1/E^{1.6}$. The spectra near 0628 of day 45 (in the same figure), the distribution is higher than $\sim 1/E^2$ for electrons in the same energy range, Another example can be seen in the outer magnetosheath during inbound pass near 1757, day 33, (upper panel of Figure 1 of *Phillips et al. [1993]).* The electron spectrum is shown even flatter. These observations of electron distributions support the above analysis which shows that the waves propagate at a rather large wave angle of about 40°.

For a whistler mode to be unstable, it is also required that the electrons maintain a certain pitch angle anisotropy [*Kennel and Petschek, 1966].* The temperature anisotropy must satisfy

$$\frac{T_\perp}{T_\parallel} > \frac{1}{1 - \frac{\omega}{\Omega_e}},$$

where $T_\perp$ and $T_\parallel$ are the perpendicular and parallel electron temperatures, respectively. From the observed peak frequency we may estimate the minimum anisotropy needed. For the interval 0520-0529, day 45, taking the wave frequency as the peak of the WFA spectra, 14.0 Hz, and the local $\Omega_e \sim$ 101,4 Hz, the minimum anisotropy required is $\sim$1 .16. We have calculated the anisotropy $T_\perp/T_\parallel$ for all wave events studied and found that the required anisotropy falls between $\sim$ 1.1 and 1.5. Such anisotropies for suprathermal electrons of $\sim$100 eV and above has been observed in the Jovian magnetosheath by Ulysses. The overall effect of the electron anisotropies in the magnetosheath (not including the boundary layer) is that $T_\perp$ generally exceeds $T_\parallel$ by a factor of 1.2 to 2 [*Phillips et* al., 1993]. We note that the main contribution to the anisotropy comes from suprathermal electrons. A typical spectrum of the electron anisotropy is (displayed in Fig 10 of *Phillips et al.* It is shown that the parallel phase space density $f(v_\parallel)$ exceeds $f(v_\perp)$ at energies below 45 cV, while $f(v_\perp)$ is dominant for electrons with higher energy.

In Table 1 we have listed some important physical quantities which resulted from our analyses of all wave intervals. The quantities include for each interval: the local electron gyrofrequency, f_{ce}, calculated from the average magnetic field strength during the interval; the peak frequency of WFA spectra for the interval and the frequency (in parentheses) of the signal captured by FES during the interval; the frequency ratio f/f_{ce}, tlhc observed ratio cB_{xy}/E_{xy}; calculated wave angle θ and the standard deviation; the calculated lower limit of anisotropy $T_\perp/T_\parallel$; the resonance energy E_{res}, and the distance of Ulysses from Jupiter,

We note that, among the 26 wave intervals, only two of them arc in the periods when Ulysses was within the magnetosphere/magnetosheath boundary layer, which is characterized by the presence of both warm electrons in the 10-100 eV range and a much hotter magnetospheric population *[Phillips et al., 1993].* Wc further note that,

during these two intervals, 1700-1710 and 1900-1915 of day 43 (Feb 12), Ulysses was actually at the magnetosheath edge of the boundary layer. For the first interval, the spacecraft entered the boundary layer from the magnetosheath at 1700, and spent about 40 min in the boundary layer before it entered the magnetosphere. For the second interval, the spacecraft entered the magnetosheath at 1910 after coming out of the magnetosphere and spent about 30 min in the boundary layer. These observations imply that the magnetopause boundary layer may not be a region favorable to the excitation of whistler mode waves. This is justified by electron observations [*Phillips et al.*, 1993] which found that the electron anisotropies within the boundary layer had the sense of $f(v_{\|}) > f(v_{\perp})$. These anisotropies prevail for all boundary layer encounters, for both the low-energy and high-energy components.

Comparison With the Earth's Lion Roars

There are similarities between the whistler waves observed in the Jovian magnetosheath and the lion roars observed in the Earth's magnetosheath. Their frequencies are a few tens of the electron cyclotron frequency, and they are likely to be generated by the cyclotron instability of anisotropic thermal electrons, as shown in this study and in *Thorne and Tsurutani* [1981], and *Tsurutani et al. [1982].* The anisotropies required are similar ($1 < T_{\perp}/T_{\|} < 2$), and the resonance energy are comparable to the electron thermal energy.

While lion roars are a characteristic feature of the Earth)s magnetosheath, which are observed throughout the magnetosheath as reported by *Smith et al.*, [1969], and *Smith and Tsurutani [1976],* the Jovian magnetosheath whistler waves observed by Ulysses occurred mostly in, presumably, the middle and outer magnetosheath, especially the region near the bow shock where there are sufficient suprathermal electrons to resonate with the waves. The propagation angles of the whistler waves in the Jovian

magnetosheath, $\sim$ 40°, are found to be larger than those of Earth's lion roars.

In the Earth's magnetosheath, lion roars were reported to occur when the ambient magnetic field decreased [*Smith and Tsurutani 19'76].* They have also been observed coupling with the mirror mode oscillations [Anderson *et al., 1982; Tsurutani et al., 1982]. In* the latter case, lion roars occurred during every decrease in the field magnitude. They arc quasi-periodic, with a typical time interval of $\sim$ 20 s between bursts. The decrease of the magnetic field lower the required resonance energy and favor the excitation of the whistler mode instability. During the outbound magnetosheath passes, Ulysses have observed strong mirror mode oscillations which lasted for more than 10 hours [*Balogh et al.,* 1992; *Tsurutani et al., 1993]* between 1400, Feb 12 (day 43), and 1100, Feb 13 (day 44). The period of the mirror mode oscillations is $\sim$1 -- 1.5 min. The plasma wave data we use are 64 s averages and are not sensitive enough to detect wave bursts during each magnetic trough. However, when the whistler wave bursts are strong enough, we have found evidence that such coupling between the mirror mode and the whistler mode occur. Figure 7 shows such examples for two periods during mirror mode oscillations. The whistle wave bursts (marked with solid dots in the figure) tend to occur when the magnetic field decreases.

Summary

We have observed electromagnetic waves in the Jovian magnetosheath during the Ulysses flyby of Jupiter. The waves are seen as burst-like emissions, They are very likely to be whistler mode waves that were generated by the anisotropic suprathermal electrons, a similar mechanism that excites the lion roars in the Earth's magnetosheath. 'l'he waves are observed more often in the middle and outer magnetosheath, especially near the bow shock, Very few are seen in the boundary layer near the magnetopause.

Properties of the waves and plasma conditions for the wave excitation are summa-

rized in Figure 8 and Table 1. In Figure 8 the quantities displayed are plotted vs the distance of Ulysses from Jupiter when the wave events were observed. The observed wave frequencies are $\sim$ 10-- 40 Hz, which are $\sim$ 0.1 --0.4 of the local electron gyrofrequency (Figure *8a*). The wave propagation angle ranges from $\sim$ 30° to $\sim$ 60°, with most of them at about 40° (Figure *8b*).

The minimum anisotropy ($T_\perp/T_\parallel$) required for these wave events is between $\sim$1.1 and 1.5 (Figure 8c). The energy of the resonant suprathermal electrons are between $\sim$40 and $\sim$ 1000 eV, with most of them below 200 eV (Figure *8d*). We noted that in Figure *8d*, if we exclude the 3 inbound events (marked with open circles), the resonance energy decreases with the distance of Ulysses from Jupiter, which may indicate that the population of suprathermal electrons are greater in the inner region than in the outer region of the magnetosheath. The required anisotropies and sufficient resonant electrons exist as observed by the Ulysses plasma experiment.

There is evidence that whistler emissions in the Jovian magnetosheath also occur coupling with the mirror mode oscillations, a phenomena similar to lion roar emissions occur in the Earth's magnetosheath.

Acknowledgments. We would like to thank R. G. Stone, the principal investigator of the URAP experiment, for the opportunity to take part in this investigation. We also thank S. J. Monson and K. Goetz of the University of Minnesota for the development of FES experiments and the interpretation of the data. We thank A. Balogh and R. J. Forsyth for providing the magnetometer data, and thank S. J. Bame for the plasma data. The authors also thank H, Friedman, P. Testerman, and D. Thayer of the University of Minnesota for their assistance in data processing. The work done at the University of Minnesota was supported by NASA under contract NAS5-31219.

TABLE 3. Summary of Physical Properties of Wave Events

Period	f_{ce} Hz	f_{WFA} (f_{FES}) Hz		f/f_{ce}	cB/E	e deg	$T_\perp/T_\parallel$	E_{res} Cv	r R_J
Inbound:									
Feb 2,92 (day 33)									
1'733	bow shock crossing								113
1820-1835	59.8	9.3	/	**0.16**	184.5	**48.8±7.3**	1.19	555.8	112.4
1925-1945	79.0	18.7	/	0.24	155,1	**39.9±12.**	1.32	329.5	**111.5**
2115-2125	91.2	14.0	/	0.15	244,0	**40.9±6.8**	**1.18**	488.4	110.3
Outbound:									
Feb 12, 92 (day 43)									
1510-1525	118,7	9.3	/	0.08	322.1	**42.4±6.6**	1.09	843.4	**83.7**
1530-1550	105.3	9.3	/	0.09	349.0	41.14-9,6	1.10	419.7	83.9
1610-1620	105.5	9.3	/	0.09	278.4	**45.3±9.7**	1.10	1134.5	84.4
1700-1710	11'7.5	18.7	/	0.16	131.2	**45.9±** 7.6	1.19	505.8	85.0
1900-1915	11.4.'7	14.0	/	0.12	75.8	**57.4±5.9**	1.14	1088.1	86.6
Feb 13, 92 (day 44)									
0755-0810	88A	18.7	(18.3)	0.21	267,0	**35.6±8.5**	1.27	91.6	96.3
0920-0935	81.4	9.3	/	0.11	263.9	47,257.3	1,12	184.5	97.4
1005-1015	93.0	18.7	(14.0)	0.20	273.8	**34.9±** 8.4	1.25	36.7	97.9
1050-1100	111.8	37.0	(36.5)	0.33	270.6	**31.7±5.4**	1.49	50.2	98.5
1115-1125	108.4	14.0	**(16.7)**	0.13	**309.2**	43.159,9	1.15	240.4	98.8
1705-1720	108.3	18.7	/	0.17	246.7	**45.6±** 5.2	1,20	114.6	103.1
1755-1812	109.2	14.0	/	0.13	**313.2**	**41.2±9.7**	1.15	121.0	103.8
2035-2100	89.3	14.0	/	0.16	306,9	**38.8±8.5**	1.19	83.2	105.8
2320-2340	99.0	9.3	/	0.09	388.1	**46.2±** 8.9	1.10	163.3	107.9
Feb 14, 92 (day 45)									
0037	bow shock crossing								108.6
0428	bow shock crossing								111.5
0505-0518	97.2	9.3	(18.3)	0.10	284.1	**40.4±5.1**	1.11	75.3	**112.1**
0520-0529	101.4	14.0	(16.7)	0.14	289.6	**37.4±6.8**	1.16	48,3	112.2
0529-0540	**98.9**	14.0	/	0.14	276.7	43.1 **±5.9**	1.16	32.8	112.4
0550-0600	90.7	9.3	(11.3)	0,10	325.5	**42.1±6.8**	1.11	361,0	**112.6**
0615-0625	94.9	18.7	/	0,20	292.8	**39.2±** 1.1	1.25	149,7	112.9
0645-0655	86,0	9.3	/	0.11	341.7	**36.1±8.2**	1.12	120.5	113,3
Feb 16, 92 (day 47)									
0400-0410	113.4	37.0	(38.3)	0.33	205.2	**38.4±4.6**	1.49	85.4	146.6
0505-0515	110.7	28.0	/	0,25	201.6	**40.0±** 4.3	1.33	125.3	147.4
0620-0630	99.2	18.7	**(18.8)**	0.19	283.2	41.64-6,3	1.23	122.1	148.3
0753	bow shock crossing								149.3

References

Anderson, R. R., C. C. Harvey, M. M. Hoppe, B. T. Tsurutani, T. E. Estman, and J. Etcheto, Plasma waves near the magnetopause, *J. Geophys. Res.*, bit 87,2082, 1982.

Balogh, A., M. K. Dougherty, R. J. Forsyth, D. J. Southwood, E. J. Smith, B. T. Tsurutani, N. Murphy, and M. E. Burton, Magnetic field observations during the Ulysses flyby of Jupiter, *Science,* 257, 1539, 1992.

Chang, D. B., Amplified whistlers as the source of Jupiter's sporadic decameter radiation, *Astrophys. J.,* 1$8(4), 1231, 1963.

Farrell, W. M., et al., Ulysses observations of auroral hiss at high Jovian latitudes, *Geophys. Res. Lett., 20, 2259, 1993a.*

Farrell, W. M., R. J. MacDowall, R. A. Hess, M. L. Kaiser, M, D. Desch, and R, G. Stone, An interpretation of the broadband VLF waves near the 10 torus as observed by Ulysses, *J. Geophys. Res.*, 98, 21177, 1993*b.*

Gurnett, D. A., and F. L. Scarf, Plasma waves in the Jovian magnetosphere, in *Physics of the Jovian Magnetosphere,* edited by A, J. Dessler, p. 454, Cambridge Univ. Press, 1983.

Kaiser, M. L., M. D. Desch, and W, M. Farrell, Clock-like behavior of Jovian continuum radiation, *Planet. Space Sci.*, in press, 1994.

Kellogg, P. J., K. Goetz, R. L. Howard, S, J. Monson, Evidence for Langmuir wave collapse in the interplanetary plasma, *Geophys. Res. Lett., 19,* 1303, 1992.

Kennel, C. F., Low-frequency whistler mode, *Phys. Fluids, 9, 2190, 1966.*

Kennel, C. F., and H. E. Petschek, Limit on stably trapped particle fluxes, *J. Geophys. Res., 71,1* , 1966.

Lengyel-Frey, D., W. M. Farrell, R, G. Stone, A. Balogh, and R, Forsyth, An analysis of whistler waves at interplanetary shocks, *J. Geophys. Res.*, in press, 1994.

Lin, N., et al., ULF waves in the Io torus: Ulysses observations, *J. Geophys. Res.*, 98, 21151, 1993

Mosier, S. R., and D. A. Gurnett, Theory of the Injun 5 very-low-frequency Poynting flux measurements, *J. Geophys. Res.*, 76, 972, 1971.

Phillips, J. L., S. J. Bame, M. F. Thomsen, B. E. Goldstein, and E. J. Smith, Ulysses plasma observations in the Jovian Magnetosheath, *J. Geophys. Res.*, 98, 21189, 1993.

Scarf, F. L., D. A, Gurnett, and W. S. Kurth, Measurements of plasma wave spectra in Jupiter's magnetosphere, *J. Geophys. Res.*, 86, 8181, 1981

Sentman, I). D., and C. K. Goertz, Whistler mode noise in Jupiter's inner magnetosphere, *J. Geophys. Res.*, 83, 3151, 1978.

Smith, E. J., R. E. Holzer, M. G. McLeod, and C. T. Russell, Magnetic noise in the magnetosheath in the frequency range 3-300 Hz, *J. Geophys. Res.*, 72, 4803, 1967.

Smith, E. J., R. E. Holzer, and C. T. Russell, Magnetic emissions in the magnetosheath at frequencies near 100 Hz, *J. Geophys. Res.*, **74,** 3027, 1969.

Smith, E. J., and B. T. Tsurutani, Magnetosheath lion roars, *J. Geophys. Res., 81,* 2261, 1976.

Stix, T. H., *The Theory of Plasma Waves*, McGraw-Hill Book Co., New York, 1962.

Stone, R. G, et al., Ulysses radio and plasma wave observations in the Jupiter environment, Science, 257, 1524, 1992*a*.

Stone, R.. G. et al., The unified radio and plasma wave investigation, *Astron. Astrophys. Supp.* ser., 92, 291, 1992*b*.

Thorne, R. M., and B. T. Tsurutani, Generation of magnetosheath lion roars, *Nature, 299, 384, 1981.*

Tsurutani, B. T., E. J. Smith, R. R. Anderson, K. W. Ogilvie, J. D. Scudder, D. N. Baker, and S. J. Bame, Lion roars and non oscillatory drift mirror waves in the magnetosheath, *J. Geophys. Res.*, *87*, 6060, 1982.

Tsurutani, B. T., D. J. Southwood, E. J. Smith, and A, Balogh, A survey of low frequency waves at Jupiter: The Ulysses encounter, *J. Geophys. Res.*, *98*, 21203, 1993.

Figure Caption

Fig. 1. The trajectory of Ulysses relative to the magnetic dipole during the flyby of Jupiter. The horizontal axis, r_{xy}, is the cylindrical radius from the center of Jupiter, and the vertical axis is the cylindrical z from Jupiter. The solid circles show the position of Ulysses for every hour from 1000 of Feb 2 to 1000 of Feb 16. The open circles mark the beginning of a day. The thick line segments indicate the periods when Ulysses was in the magnetosheath and magnetopause boundary layer,

Fig. *2a,* The magnetic field intensity (in log scale) measured in the spin plane in 5 high band channels of WFA (the central frequency of the channels are 9.3, 14.0, 19.0, 28.0, and 37.0 Hz) for days 33 to 35, 1992, during the inbound pass. The intervals when Ulysses was in the Jupiter's magnetosheath region arc marked with solid bars in the top pane], The vertical dotted lines mark the time of bow shock crossing, and the period when Ulysses was in the solar wind is labeled with 'SW'. The periodic square-wave-like enhancements most clearly seen in the 37 Hz channel arc interference from other instruments.

Fig. *2b.* The same as Fig. 2a but for days 43 to 47, 1992, during the outbound pass.

Fig. 3 u. Time variation of magnetic wave power density in log scale from the lowest 4 channels of WFA high-band data for the period of 0400-0800, Feb 14 (day 45), 1992. The intervals selected for detailed analysis are marked with solid bars.

Fig. *3b.* The same as 3a but for electric wave power.

Fig. 3c. Spectra of spin plane electric (left) and magnetic (right) wave power for the period from 0520 to 0529 UT, Feb 14, 1992, The upper panel for each component is

the logarithm of the relative intensity. In the lower panels the logarithm of the power density is shown (solid lines) along with the instrument background noise (dashed lines).

Fig. 3*d*. FES record of rectified magnetic waves at frequency of ~ 16 Hz over a 1024 mscc period ended at 0520:27 of Feb 14, 1992.

Fig. *4a*. The same as Fig. *3a* but for channels between 14 and 37 Hz and for the period of 0300-0700, Feb 16 (day 47), 1992.

Fig. 4*b*. The same as 4*a* but for electric wave power.

Fig. 4c. The same as Fig. 3*c* but for the period from 0400 to 0410 UT, Feb 16, 1992.

Fig. *4d*. FES record of rectified magnetic waves at frequency of ~ 38.3 Hz over a 1024 msec period ended at 0405:30 of Feb 16, 1992.

Fig. 5. Transformation between the wave coordinate system and the spacecraft coordinate system.

Fig. 6. The wave angle derived for period 0520-0529, Feb 14 (day 45), 1992. The central frequency of the channel an alyzed is 14.0 Hz. The average wave angle for this interval is 37.4° ± 6.8°.

Fig. 'i'. Whistler mode waves (thick lines) during two periods of mirror mode oscillations of the ambient magnetic field (thin lines) for periods 1430- 1730, Feb 12, (upper panel), and 1400-1800, Feb 13 (lower panel). The whistler wave bursts That occur at magnetic field minima are marked with the dots.

Fig. 8. Wave parameters plotted vs the distance of Ulysses from Jupiter: (a) The frequency ratio f/f_{ce}; (b) The wave angle with the standard deviation; (c) The required minimum anisotropy $T_\perp/T_\parallel$; and (d) The resonance energy of electrons.

The data for 3 inbound events are marked with the open circles, while the solid circles are for outbound events.

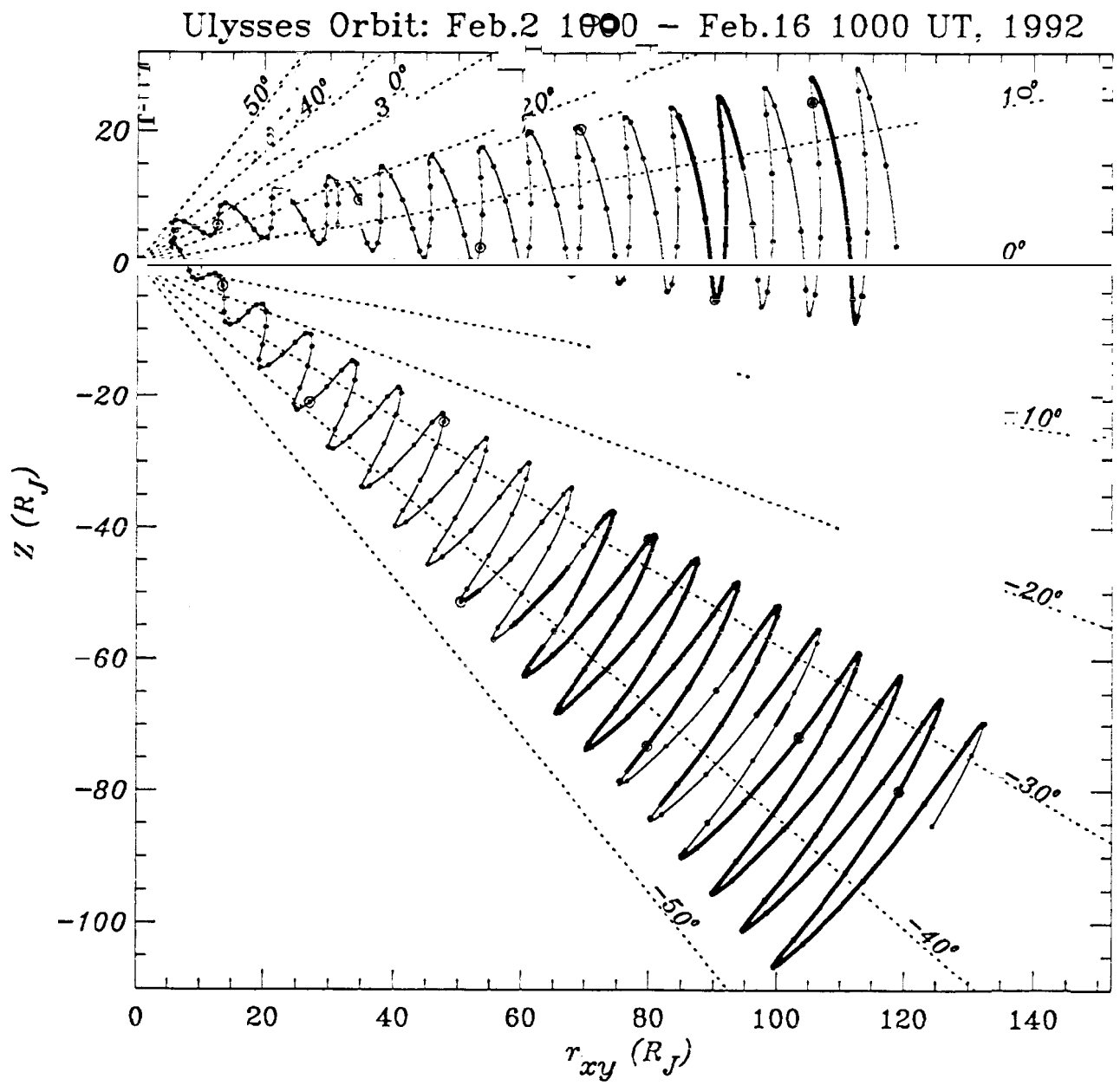
Ulysses Orbit: Feb.2 1000 – Feb.16 1000 UT, 1992
50°
40°
30°
20°
10°
0°
-10°
-20°
-30°
-40°
-50°
Z (R_J)
r_xy (R_J)
20
0
-20
-40
-60
-80
-100
0
20
40
60
80
100
120
140

Figure 1

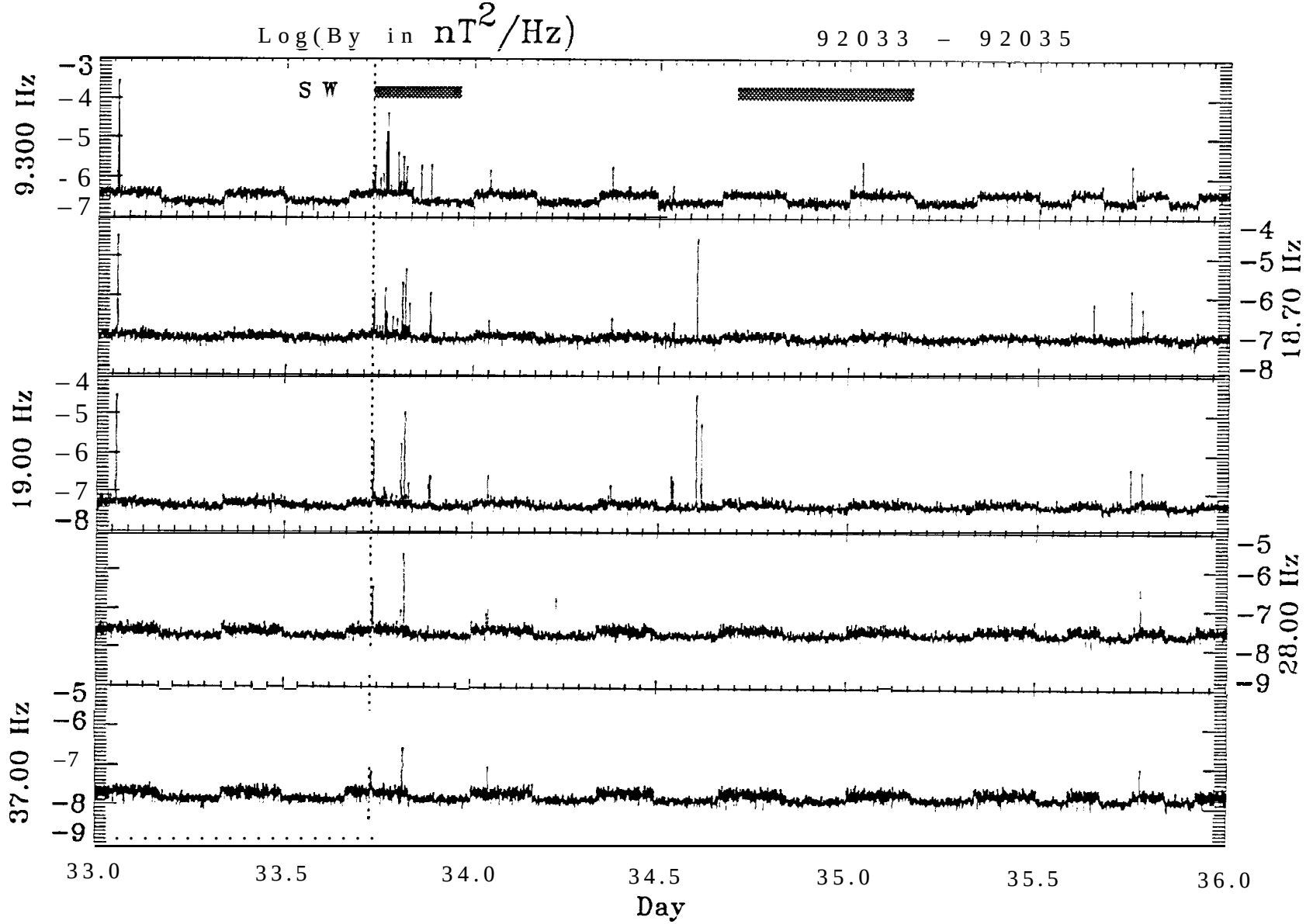
Log(By in nT²/Hz)
92033 – 92035
SW
9.300 Hz
18.70 Hz
19.00 Hz
28.00 Hz
37.00 Hz
33.0
33.5
34.0
34.5
35.0
35.5
36.0
Day

Figure 2(a)

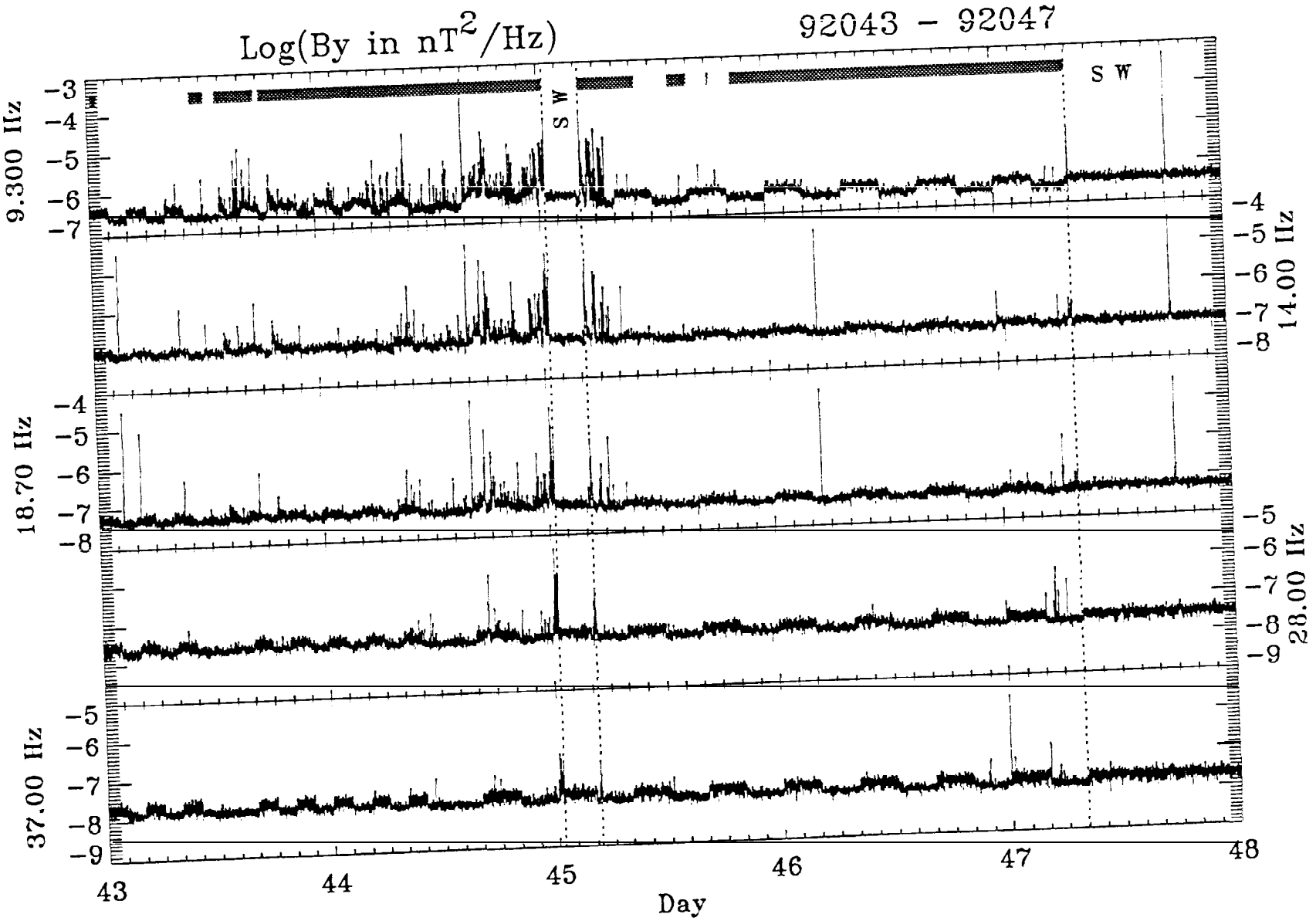
Log(By in nT^2/Hz)
92043 - 92047
S W
S W
9.300 Hz
14.00 Hz
18.70 Hz
28.00 Hz
37.00 Hz
Day
43
44
45
46
47
48

Figure 2(b)

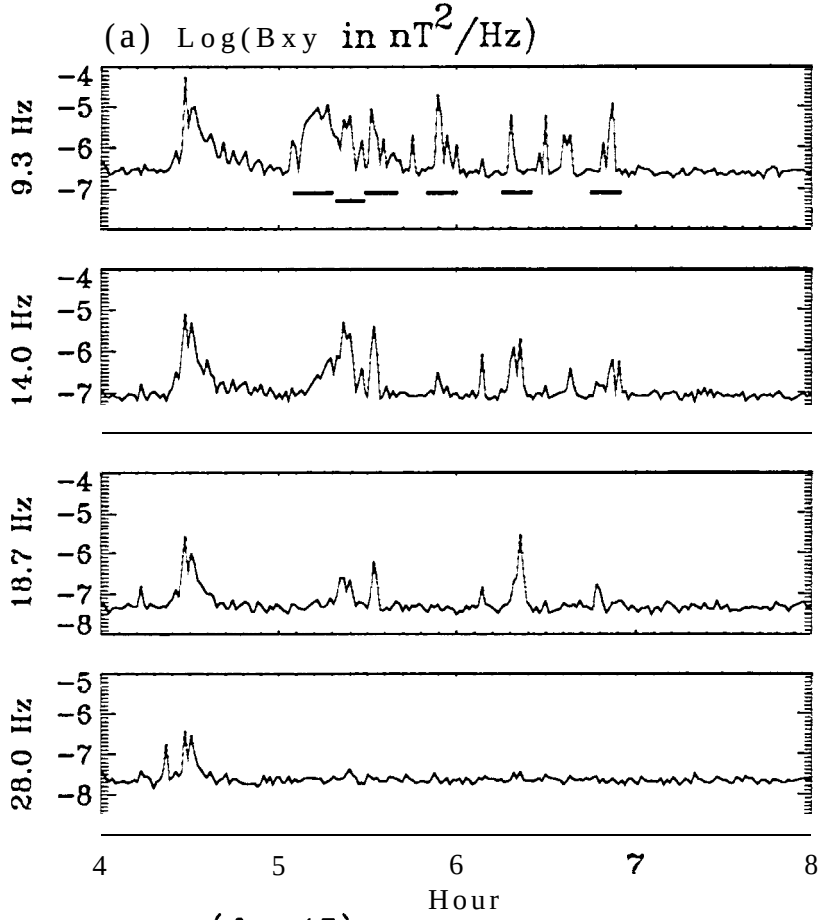

Feb 14. 1992 (day 45)

Figure 3a

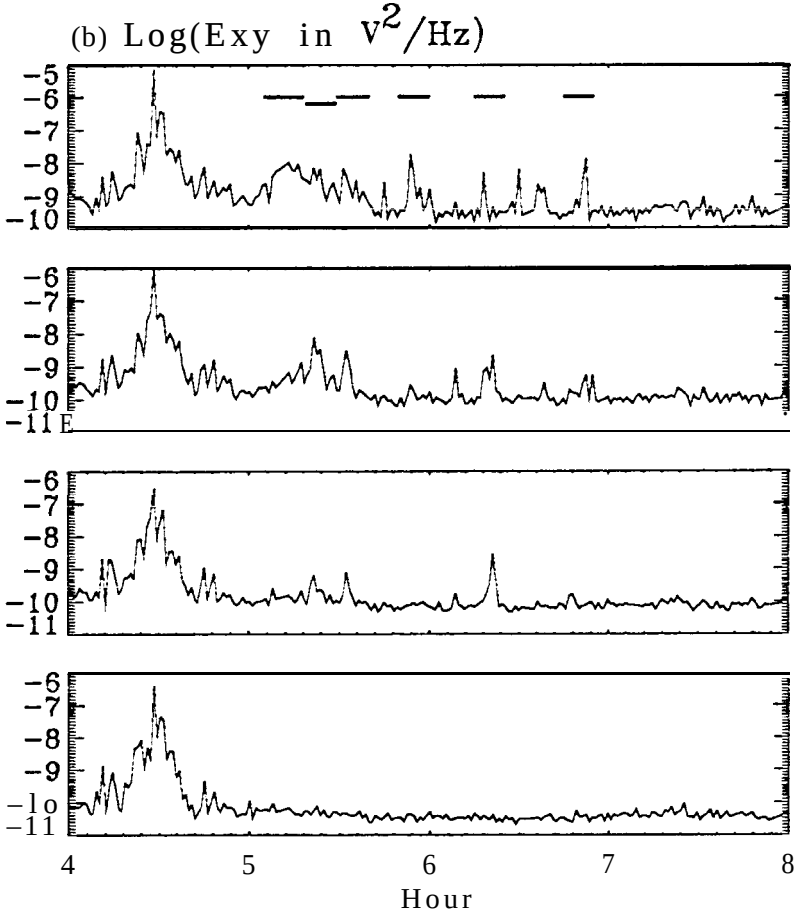

Figure 3b

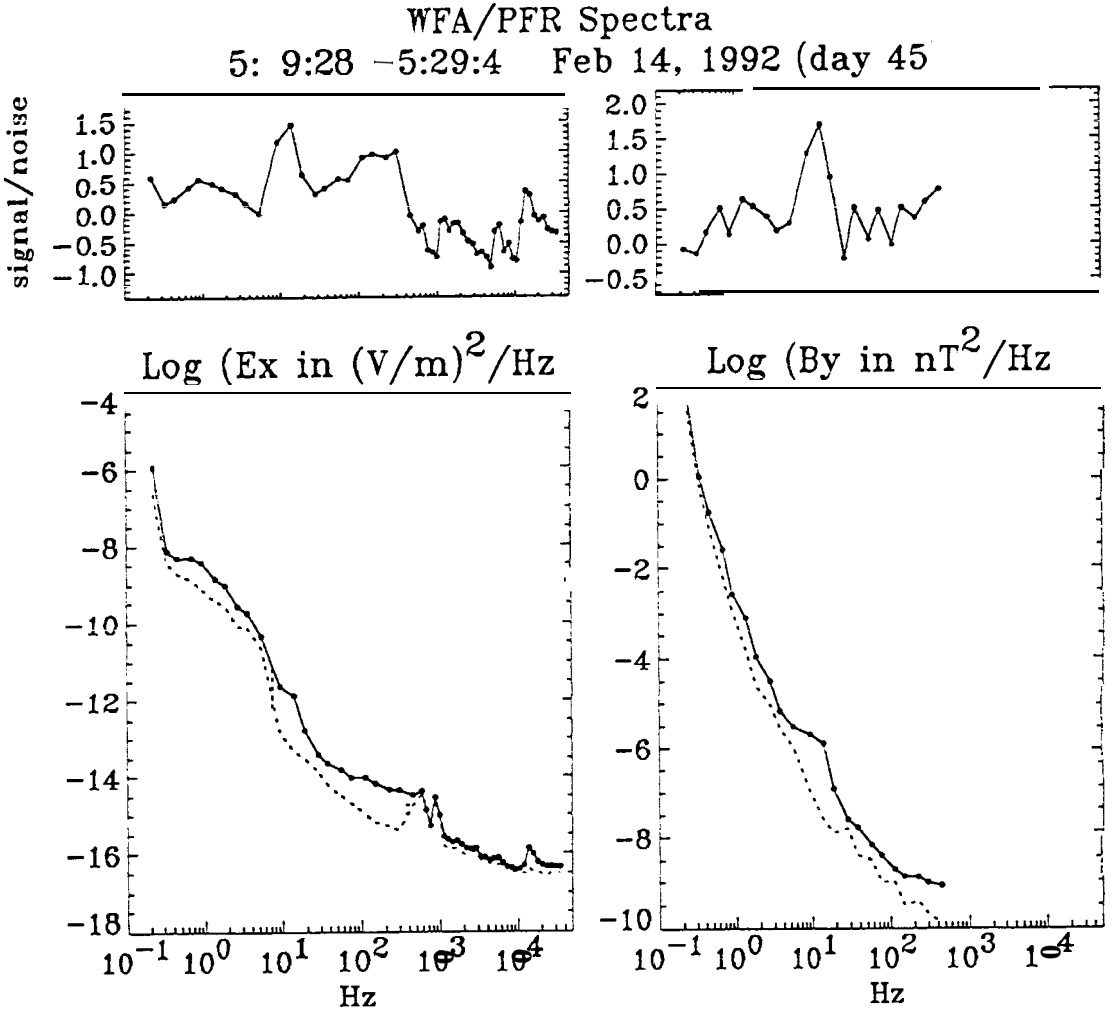
WFA/PFR Spectra
5: 9:28 -5:29:4 Feb 14, 1992 (day 45
signal/noise
1.5
1.0
0.5
0.0
-0.5
-1.0
2.0
1.5
1.0
0.5
0.0
-0.5
Log (Ex in (V/m)^2/Hz
-4
-6
-8
-10
-12
-14
-16
-18
10^{-1} 10^0 10^1 10^2 10^3 10^4
Hz
Log (By in nT^2/Hz
2
0
-2
-4
-6
-8
-10
10^{-1} 10^0 10^1 10^2 10^3 10^4
Hz

Figure 3c

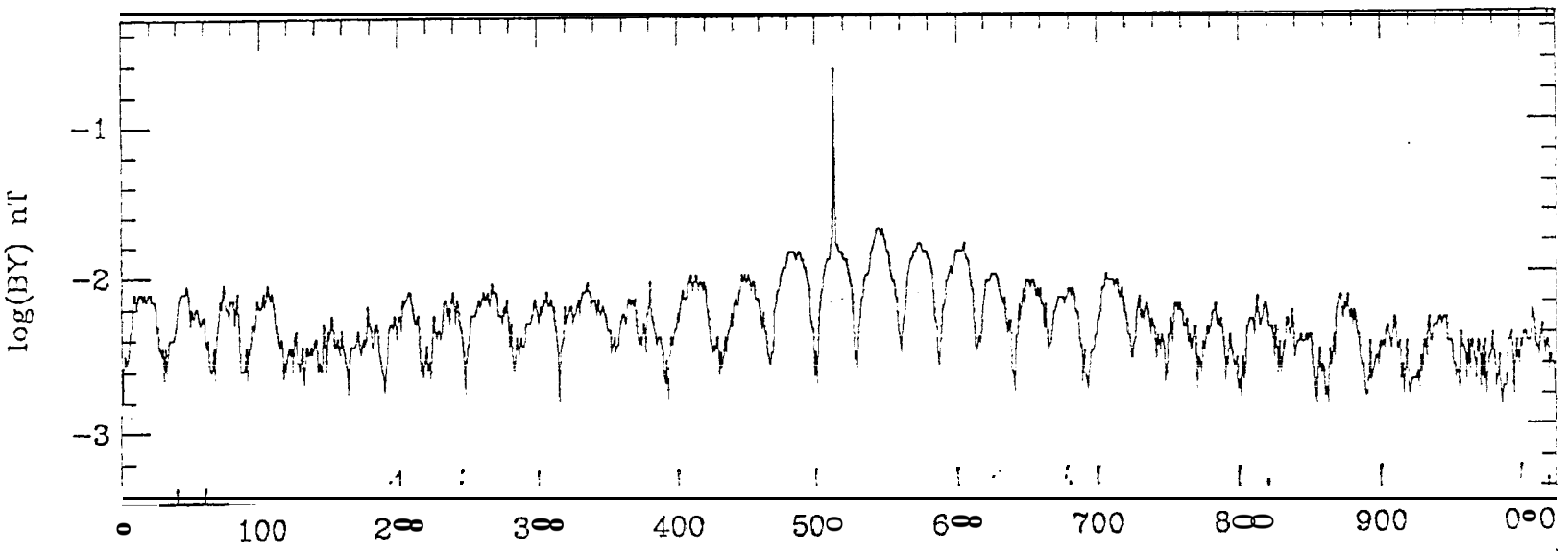

Figure 3d

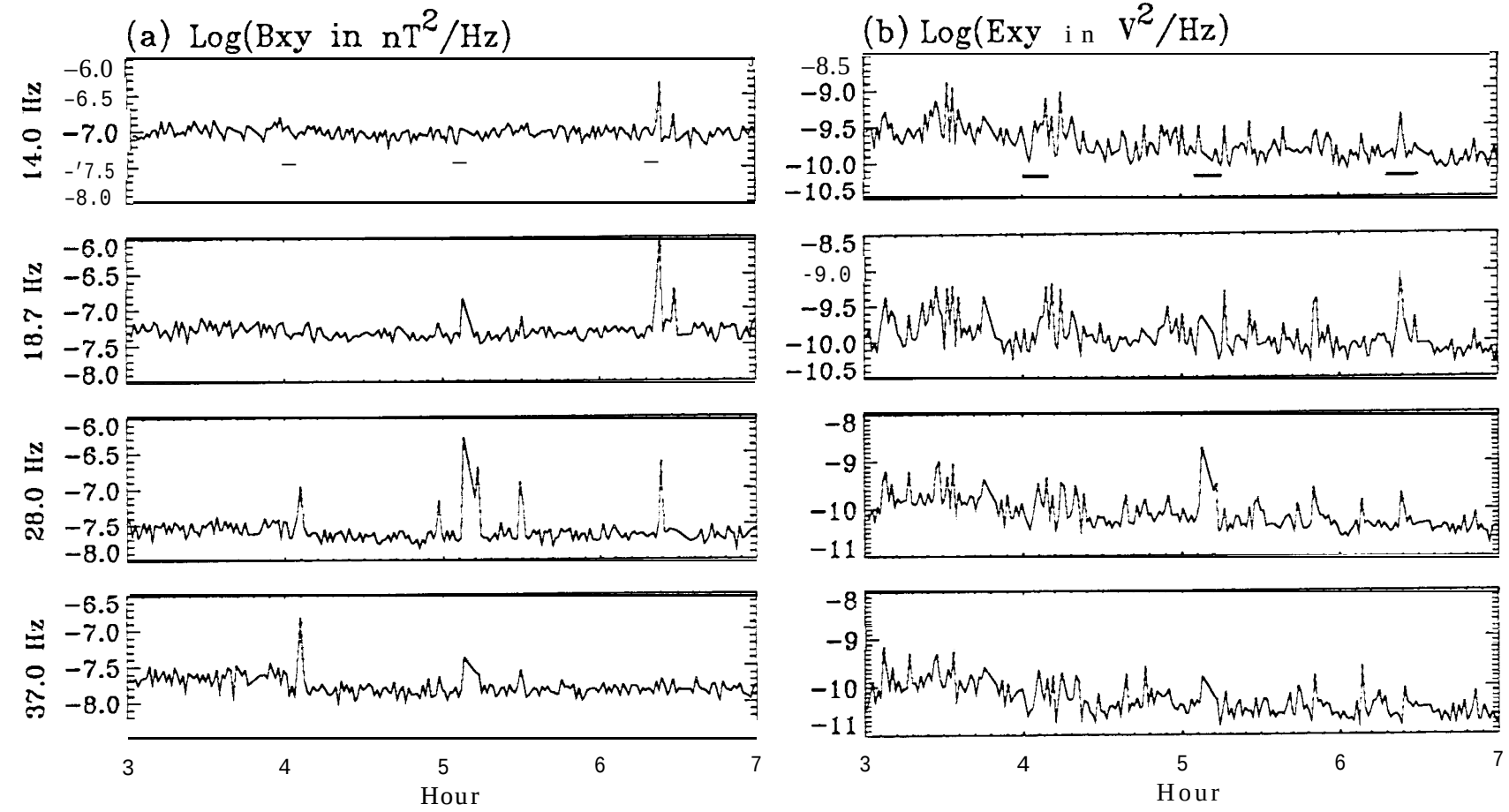

Feb 16, 1992 (day 47)

Figure 4a

Figure 4b

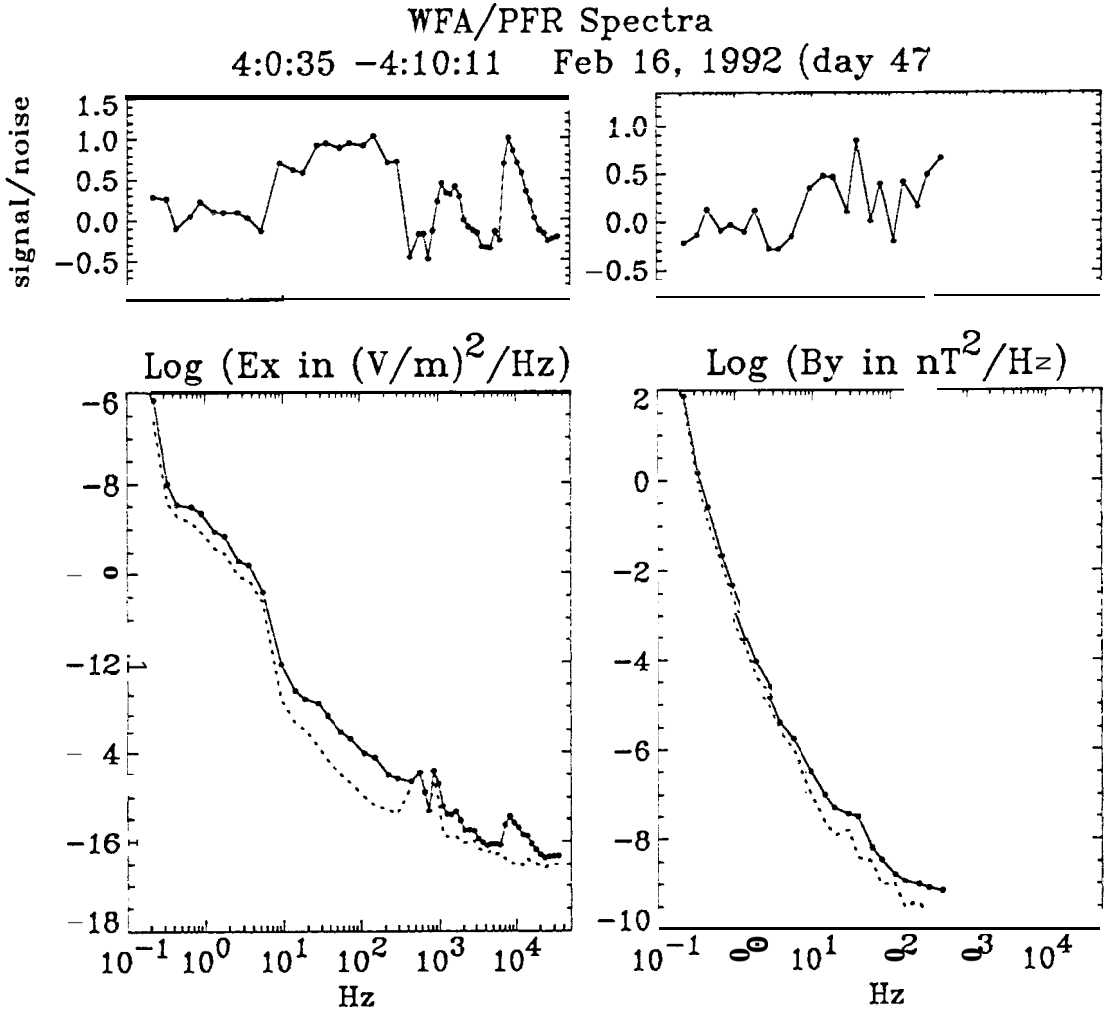
WFA/PFR Spectra
4:0:35 -4:10:11 Feb 16, 1992 (day 47
signal/noise
1.5
1.0
0.5
0.0
-0.5
1.0
0.5
0.0
-0.5
Log (Ex in (V/m)^2/Hz)
Log (By in nT^2/Hz)
-6
-8
-12
-16
-18
2
0
-2
-4
-6
-8
-10
10^{-1} 10^0 10^1 10^2 10^3 10^4
Hz
10^{-1} 10^0 10^1 10^2 10^3 10^4
Hz

Figure 4c

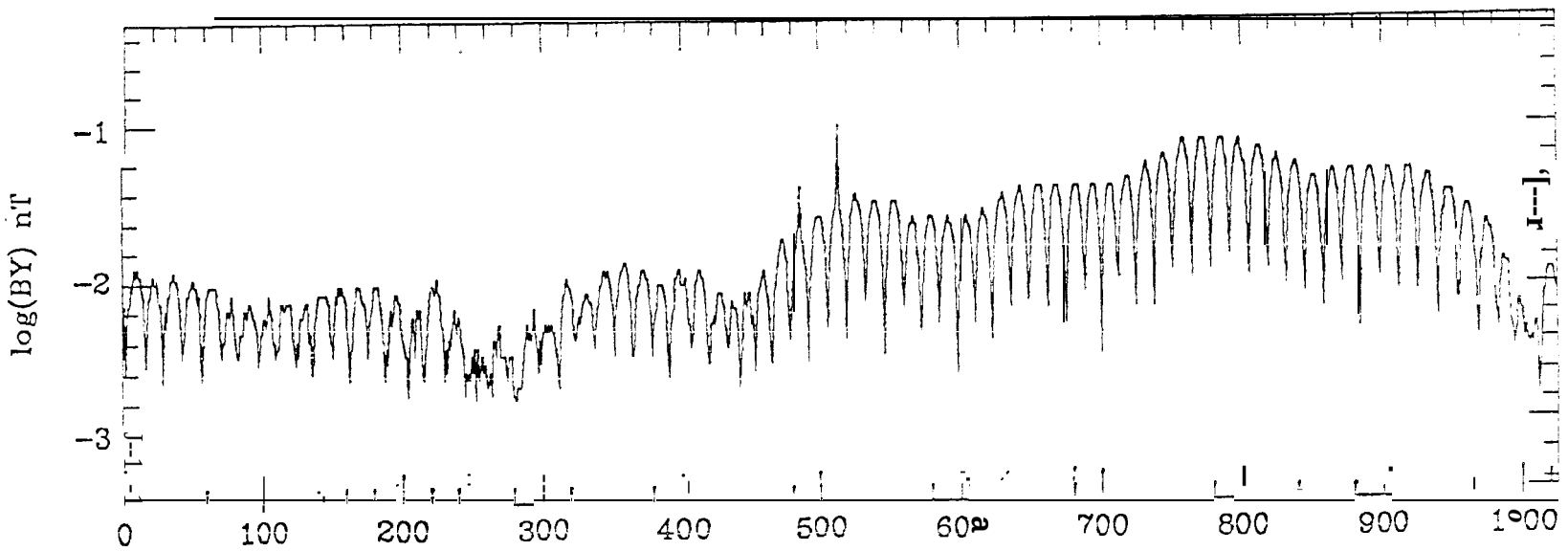

Figure 4d

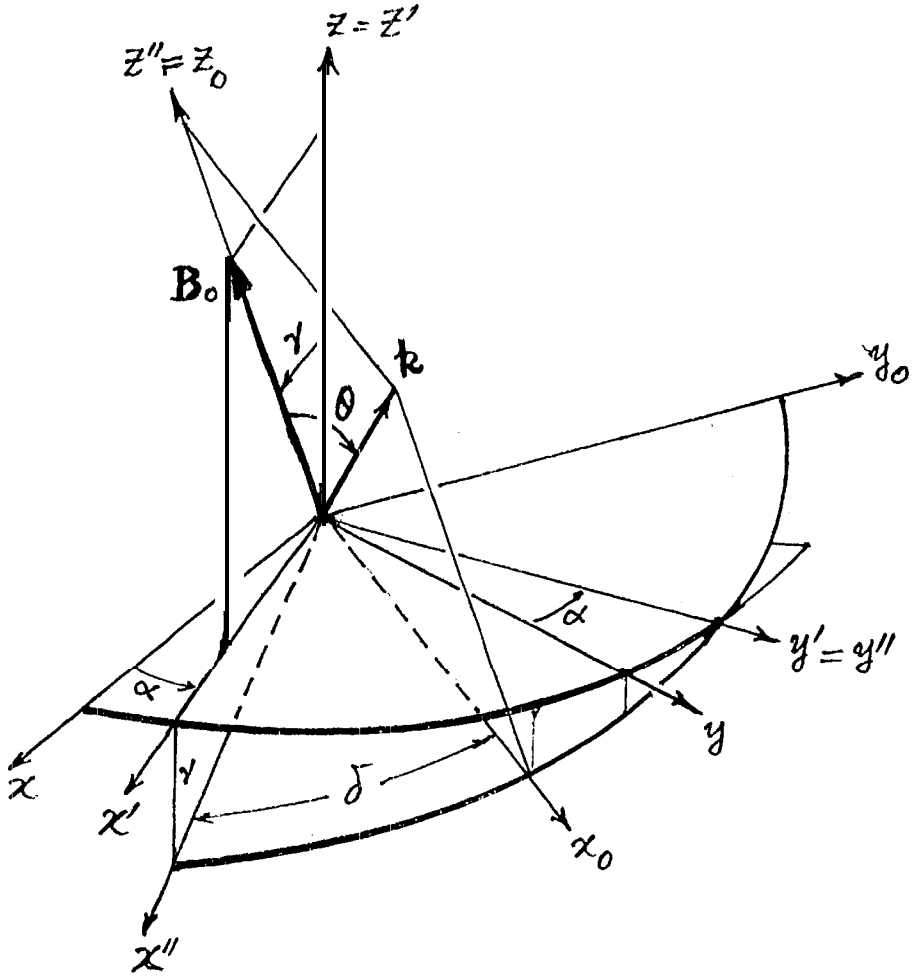

Figure 5

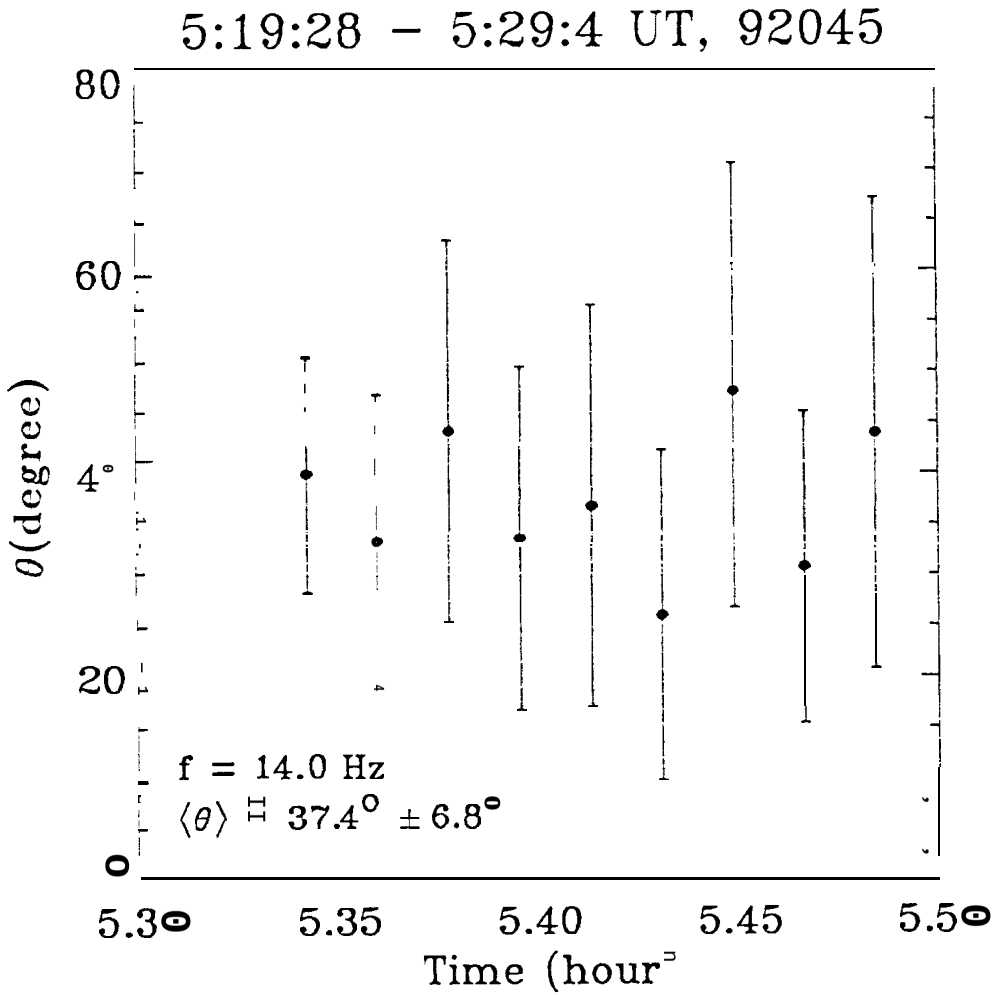
5:19:28 – 5:29:4 UT, 92045
80
60
4°
20
0
θ(degree)
f = 14.0 Hz
⟨θ⟩ = 37.4° ± 6.8°
5.30
5.35
5.40
5.45
5.50
Time (hour)

Figure 8

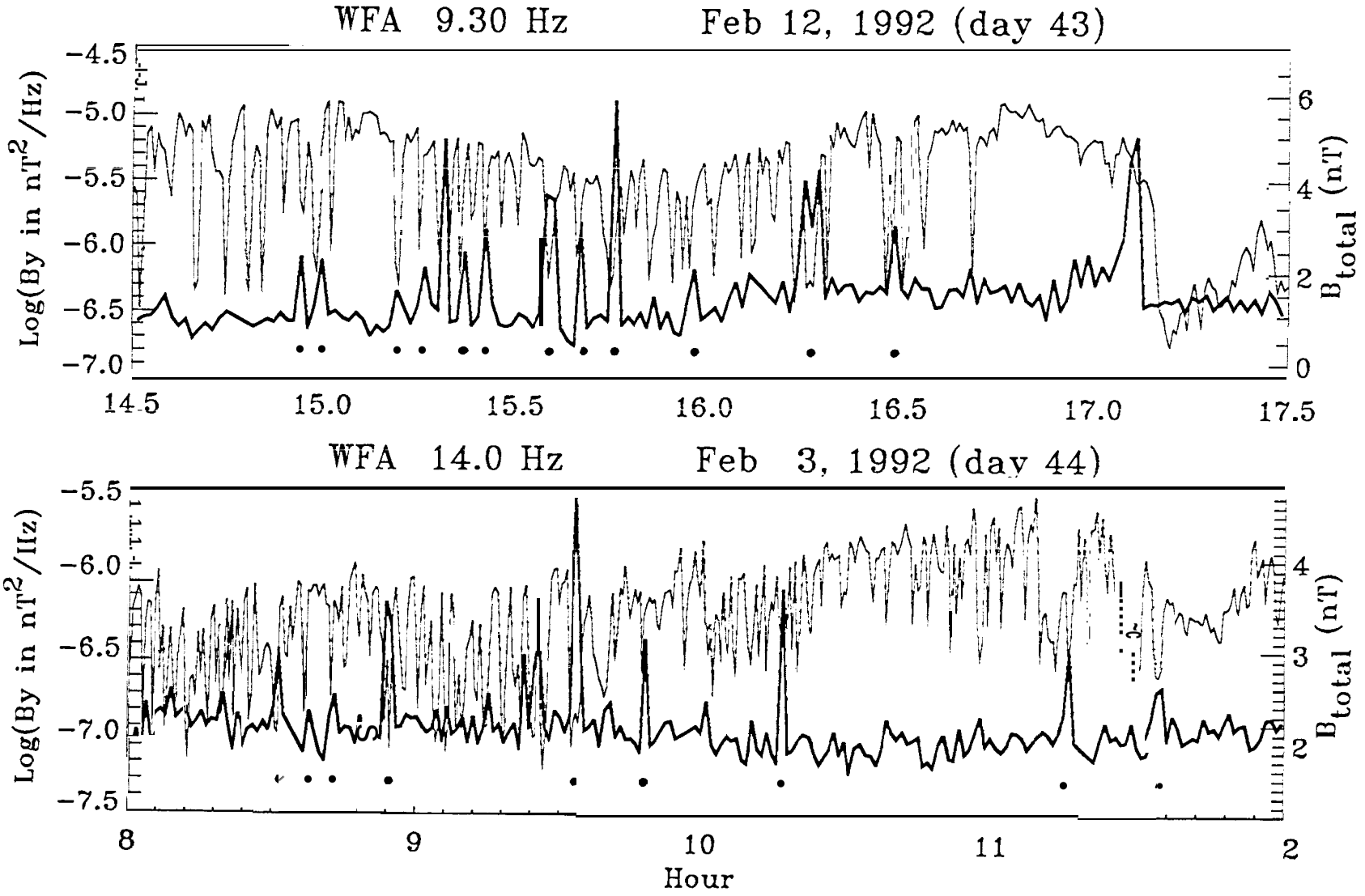
WFA 9.30 Hz
Feb 12, 1992 (day 43)
Log(By in nT^2/Hz)
B_{total} (nT)
WFA 14.0 Hz
Feb 3, 1992 (day 44)
Log(By in nT^2/Hz)
B_{total} (nT)
Hour

Figure 7

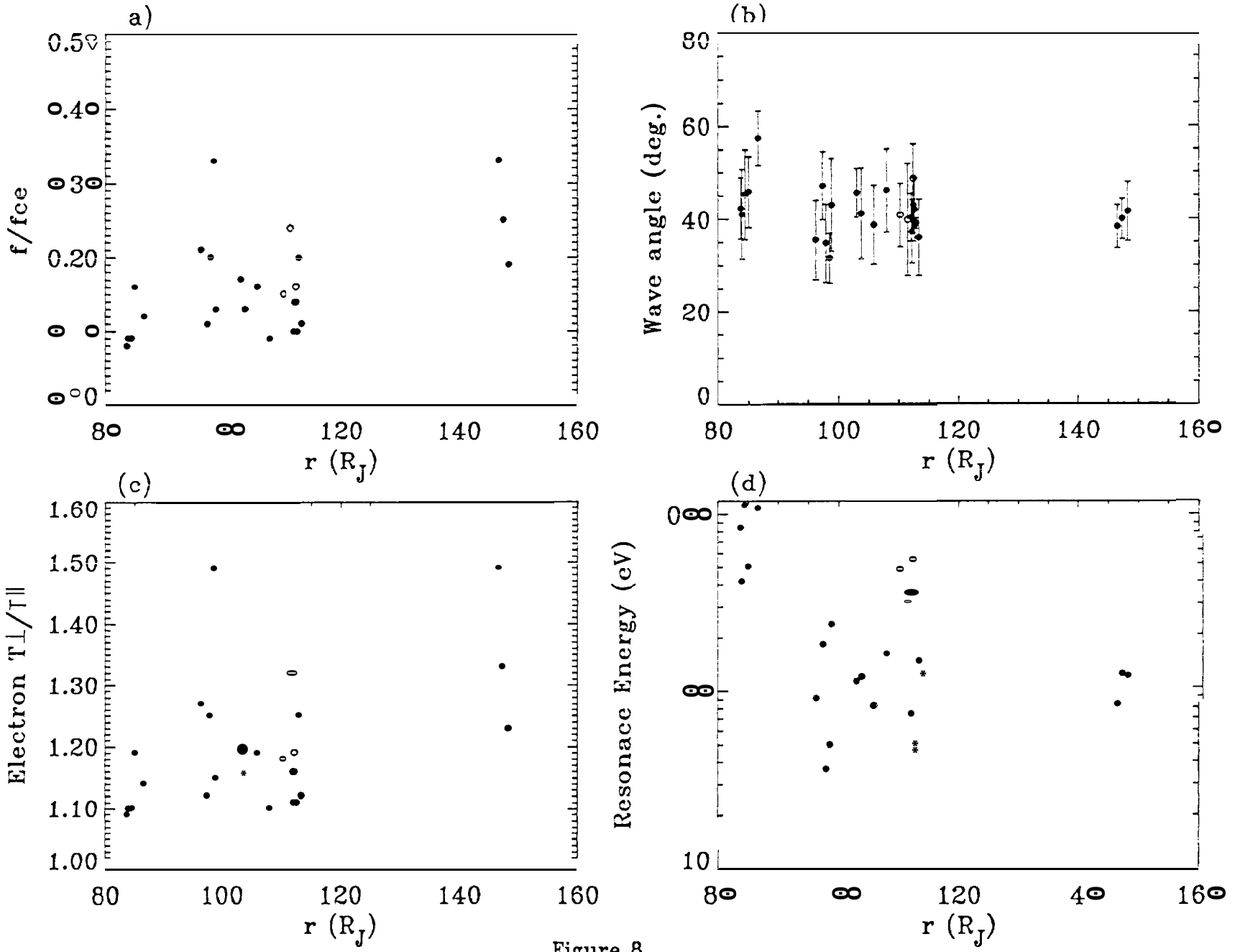
a)
f/fce
r (R_J)
(b)
Wave angle (deg.)
r (R_J)
(c)
Electron T⊥/T||
r (R_J)
(d)
Resonace Energy (eV)
r (R_J)

Figure 8